PIEZO STACK ACTUATORS IN FLEXIBLE STRUCTURES: EXPERIMENTAL VERIFICATION OF A NONLINEAR MODELING AND IDENTIFICATION APPROACH

Alexander Schirrer, Martin Kozek, Christian Benatzky
Institute of Mechanics and Mechatronics
Division of Control and Process Automation
Vienna University of Technology
Austria
alexander.schirrer@tuwien.ac.at

Abstract

Piezoelectric actuators are applied in many mechatronic disciplines, from combustion engine injection systems to active structure vibration attenuation. This paper describes a nonlinear piezo stack actuator modeling and identification approach for flexible structure actuation. The piezo's inherent hysteresis behaviour is modeled by the widely applied Preisach model and is identified in the structure-mounted configuration using a frequency-averaging technique to mask out frequency-dependent structure response in the hysteresis identification. Moreover, linear structure identification, simulation, and experimental results are given. The experimental setup under study is a large-scale stack actuator, console-mounted on a steel truss with a low first natural frequency at about $20\mathrm{Hz}$. This system is used for model validation and to measure the performance of the system inversion, which can be seen as feed-forward control method. Feedback control can subsequently be supported and enhanced by eliminating the system nonlinear behaviour with the inverse hysteresis model, improving the control system's performance.

Key words

piezo actuators, Preisach hysteresis model, non-linear identification

1 Introduction

Piezoelectric stack-type actuators have distinct characteristics, such as high force generation at low stroke lengths, that make them suitable for applications in stiff structures or fast systems, such as vibration control of flexible mechanical structures. Using the reciprocal piezoelectric effect, stack-type piezo actuators expand due to an applied input-voltage. If the actuator is mounted in a flexible structure, corresponding forces are generated, which depend both on the actuator's and the structure's bulk stiffness, but as well on the vibration state of the structure. In this paper, the focus is drawn on the nonlinear hysteresis behaviour observed in the actuator's voltage - force relation.

As is pointed out in (Mayergoyz, 1991, p.4), ”the physical origin of hysteresis is the multiplicity of metastable states”. For a piezoelectric material, this can be related to the occurrence of polarization domain switching at changing voltage.

The present study considers a piezo stack-type actuator mounted in a flexible structure. First the modeling approach will be presented, followed by a discussion on implementation and identification aspects of the widely-applied Preisach hysteresis model for our system. Then, experimental results regarding system and hysteresis parameter identification and the measured performance of hysteresis inversion will be given and followed by a concluding remark.

Many piezo actuator hysteresis modeling approaches exist, see (Ge and Jouaneh, 1996), (Hu and Mrad, 2003), (Hughes and Wen, 1997), (Mrad and Hu, 2002), (Song and Li, 1999), and (Yu *et al.*, 2002). The most frequently used model is the Preisach-model, which was originally proposed and mostly applied for magnetic hysteresis phenomena. However, it proved also suitable to describe many other types of hysteresis, such as those observed in piezoelectric materials. A comprehensive study on Preisach-type models and their extensions is given in (Mayergoyz, 1991).

2 Nonlinear model of piezo actuator in flexible structure

The considered piezo actuator is mounted in a console on a steel truss as flexible structure. Its generated force can be modeled by two effects. Assuming the actuator to be freely expandable, an applied input voltage U causes it to elongate by x_U (termed ”free elongation”).

However, due to its mounting in the flexible structure, the appearing reaction force F acts on the actuator and thereby compresses it again by x_F (see Fig.1). While these relations can be modeled linearly at small voltage, hysteretic nonlinear behavior is visible at high input amplitudes for the voltage - elongation or force relations. The widely-applied Preisach hysteresis model is chosen in this work.

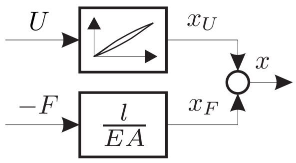

Figure 1. Nonlinear piezo model

3 The Preisach hysteresis model and its implementation

In the following, a short overview on the Preisach formulation using Everett surfaces or maps is given. For a detailed and formal treatment, see (Mayergoyz, 1991) and more recent survey articles.

3.1 The classical Preisach model - a short overview

The classical Preisach model is able to describe static general hysteresis behaviour if two main properties are fulfilled: the wiping-out property (i.e. only the last dominating extremal input values have an effect on the output, no other / earlier inputs) and the congruency property (minor loops of the same input variation are of the same shape). The hysteresis is modeled by a weighted parallel connection of simple 2-point relays as ”hysterons”. The hysteresis-inherent signal memory is essentially reduced to the dominating extremal values (minima and maxima) of the input signal $u(t)$, which thus entirely define system behaviour. The hysteresis output is described by a weighted integral of a function $\mu(u_\alpha, u_\beta)$ (often termed ”Preisach function”) over the parameter domain (u_α, u_β):

$$f(t) = \iint_{u_\alpha \geq u_\beta} \mu(u_\alpha, u_\beta)\gamma_{u_\alpha u_\beta} u(t) du_\alpha du_\beta, \quad (1)$$

where $\gamma_{u_\alpha,u_\beta}$ is the simplest hysteresis operator, represented by a rectangular loop (a 2-point relay switching ”up” at u_α and ”down” at u_β, see e.g. (Mayergoyz, 1991)). The weighting $\mu(u_\alpha, u_\beta)$, the Preisach function, has to be determined directly or indirectly through measurements of a real system. So-called ”first-order descent” (FOD) curves have to be measured, which consist of a monotonous increasing branch from the minimal input value $u_{\min}$ to u_α, yielding a final output value of f_α, as well as a monotonous decreasing branch from u_α to $u_\beta \leq u_\alpha$ with corresponding output $f_{\alpha\beta}$. In the parameter space (u_α, u_β) the so-called Everett surface is defined as:

$$E(u_\alpha, u_\beta) = \frac{1}{2}\left(f_\alpha - f_{\alpha\beta}\right) \quad (2)$$

Due to symmetry assumptions it is sufficient to limit the measurements to the triangle $T_{u_\alpha,u_\beta} : u_{\min} \leq u_\alpha \leq u_{\max}, u_{\min} \leq u_\beta \leq u_\alpha$. The connection between the Everett surface and the Preisach function is

$$E(u_\alpha, u_\beta) = \iint_{T_{u_\alpha,u_\beta}} \mu(u_\alpha, u_\beta) du_\alpha du_\beta \quad (3)$$

and

$$\mu(u_\alpha, u_\beta) = -\frac{\partial^2 E(u_\alpha, u_\beta)}{\partial u_\alpha \partial u_\beta} = \frac{1}{2}\frac{\partial^2 f_{\alpha\beta}}{\partial u_\alpha \partial u_\beta}. \quad (4)$$

These relation would in principle suffice for experimentally determining $\mu(u_\alpha, u_\beta)$ at given locations, but evaluating the double integral is computationally expensive, and differentiating measured data twice amplifies ever present measurement noise drastically. An elegant method, avoiding all numeric calculus, is presented in (Mayergoyz, 1991, p.32-35) and gives the result, that the current output value $f(t)$ can be calculated as a sum of Everett values of the present input and the past dominating extremal input values.

3.2 Identification issues and shaping of FOD curves

Using (2), the Everett surface can be meshed and identified using an appropriate input sequence. While in the classical static Preisach formulation the only requirements to these curves are their piece-wise monotonicy and a defined input history, the real piezo hysteresis is expected to include slight dynamic effects (drifts, creep). For a vibration control application, typically a certain, small frequency range is of interest, so when using a simple static hysteresis model, it should be identified in or near this operating frequency range. This can be accomplished by defining the FOD signal peak rise and fall times appropriately. A simple signal shape choice is shown in Fig.2. However, since we seek to identify the hysteresis behaviour in the structure-mounted configuration, the triangular shape is not suitable since it strongly excites structural vibration modes. As shown in the result section, this leads to non-physical artifacts in the Everett surfaces and thus deteriorates modeling quality. For this reason, we chose a smooth signal shape as in Fig.3 with good results - the structural modes are much less excited, artifacts are virtually eliminated. Additionally, we averaged over the retrieved Everett surfaces from varying peak duration / frequency FOD measurements. These measures enable one to retrieve physically plausible data of the behaviour of the hysteretic plant, while masking out structural dynamic effects sufficiently. This can be used advantageously in installed plants for non-linear hysteresis subsystem identification.

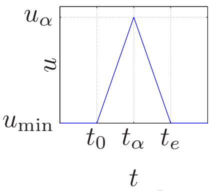

Figure 2. Simple triangular FOD curve shape

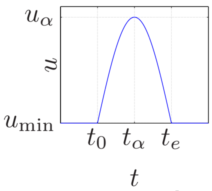

Figure 3. Smooth reversal sine FOD curve shape

Starting from a minimal voltage $u_{\min}$, the signal is increased to a voltage u_α and then decreased to $u_\beta < u_\alpha$. The output value $f_{u_\alpha u_\beta}$ and its parameter space coordinates (u_α, u_β) constitute the FOD curve.
In order to measure many FOD curves efficiently, one such signal peak for each value of u_α is generated and the system answer during the falling signal edge (decreasing u_β) is recorded.
The hard signal limitation at $u_{\min}$ and the corresponding non-smooth signal shape at the start and end times of the peak excites all frequencies, which is more severe with shorter peak times. This limits the identification speed, since it requires breaks between the peaks to let the structure vibrations attenuate sufficiently. Also, dynamic sensor effects such as the discharging of piezo patch sensors have to be considered.

3.3 Preisach model inversion

As outlined e.g. in (Kozek and Gross, 2005), the Preisach model can be inverted by calculating an inverse Everett surface, defined by

$$E_{\text{inv}}(f_\alpha, f_{\alpha\beta}) = u_\alpha - u_{\alpha\beta}. \tag{5}$$

Having identified the hysteresis before and computed the Everett surface for it, this can now be used to compute a mesh of inverse Everett values and the inverse surface can be entirely defined by interpolation. The computation of the inverse system output can be done using the same algorithm, thereby using the inverse Everett surface values.
The inverted hysteresis model can be used as feedforward compensation of the hysteresis nonlinearity. This would ideally lead to a linear actuator transfer function of 1, if the hysteretic system strictly obeyed all prerequisites of the Preisach model such as being static and fulfilling the wiping-out and the congruency properties.

4 Experimental results

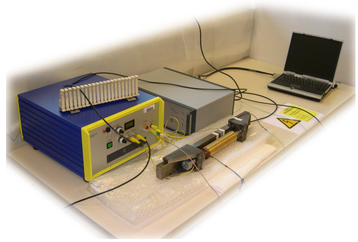
Figure 4. Actuator mounted in a console on steel truss

The piezo high-voltage stack-type actuator under study is a Piezomechanik PSt 1000/35/200 V45 and built of PZT-ceramics material. It can generate a blocking force of 50kN and can reach a maximum free elongation of $200\mu\text{m}$. As flexible structure we used a steel truss / console configuration, equipped with piezo force and strain sensors (Kistler SlimLine ForceLink 9173B, Smart Materials MFC M 2814 P2). The experiment setup can be seen in Fig.4, steel extensions of $1m$ length each were welded to the console's ends later to reduce the natural frequencies. In this setup, the actuator can generate a force of around 4kN, and the first structure vibration mode lies at around 20Hz.
In order to design a vibration control system using control forces that are generated by the actuators, the transfer behaviour from actuator voltage to generated force is of special interest. The experimental results thus concentrate on this output quantity.

4.1 Linear System Identification

Figure 5 shows a magnitude transfer function estimate for the entire flexible system, from the driving voltage U to the force F. Also, a 12th-order ARMAX model has been fitted to the data, showing good agreement. The first natural frequency lies low at around 20Hz. For the identification process, the system was excited by a white noise input voltage signal of high variance; the measurements were taken at a sampling rate of 1000Hz.

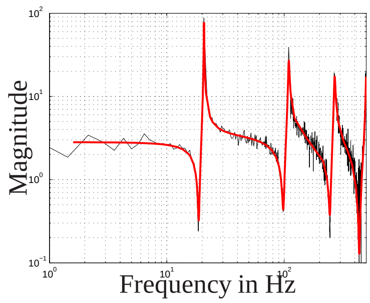

Figure 5. Identified (linear) system response and 12th-order ARMAX model: Voltage - Force

4.2 Non-linear system response to harmonic input

Figures 6, 7, and 8 show the actuator gains from voltage to force / elongation for various frequencies and amplitudes of harmonic input signals. One can observe that the measured frequency range is uncritical (only little change across frequencies). However, the input amplitude does have a strong influence on the system gain - large signals are amplified more than small ones. This, together with inherent flexible structure vibration feedback make a closed-loop actuator force control solution necessary for active vibration control. Accurate modeling, identification and inversion-based linearization of the actuator's nonlinearity can therefore lead to a more effective linear control design later on.

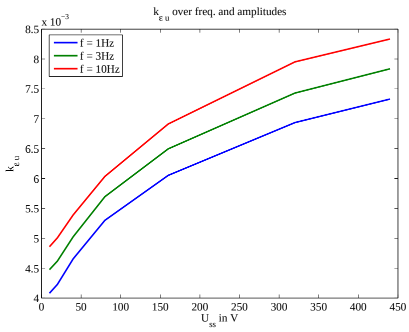

Figure 6. Actuator gain: voltage to elongation, varying input amplitudes and frequencies

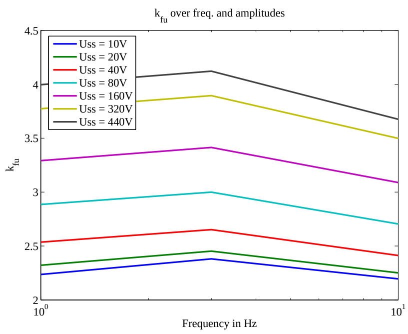

Figure 7. Actuator gain: voltage to force, varying input amplitudes and frequencies

4.3 Preisach model parameter identification

Signals realizing the FOD curves for 50 values of u_α were generated, spanning across the entire working voltage range of the actuator ($100 - 900$V). Upon driving the system with this input signal, the output at the descending slope of each FOD curve yielded the respective $F_{\alpha\beta}$ value, which was used to compute the Everett surface of the Preisach model. The sensor signals were sufficiently noise-free, so no further output signal post-processing was necessary.

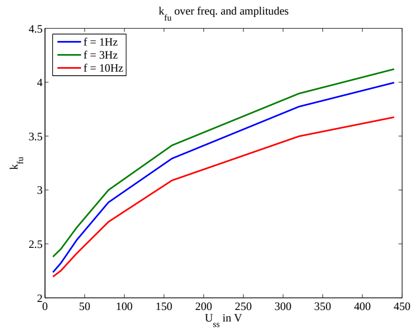

Figure 8. Actuator gain: voltage to force, varying input amplitudes and frequencies

As discussed in section 3.2, the FOD curve shape was tuned in order to avoid excessive excitation of structure modes. Figure 9 shows the Everett surface retrieved using a simple FOD shape (triangular wave). The non-smooth reversal point at u_α excites higher structure modes, which deteriorate the measurement and lead to the artifacts visible in Fig.9. This can be avoided by using smooth FOD curve shapes (sine half waves).

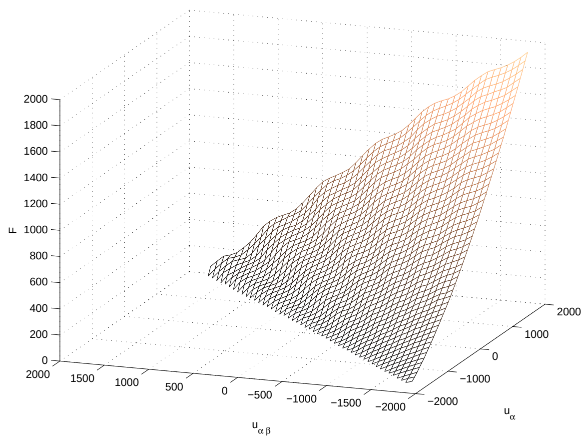

Figure 9. Measured Everett-surface for $U - F$ relation, distorted by a structure mode

Figure 10 shows the final Everett surface, using the sine FOD curve form and averaging over several runs with FOD peak time variation. The retrieved Everett surface is strictly positive and strictly monotonous and thus valid. Figure 11 is the computed inverse surface which is used for the inversion feed-forward test measurement below.

4.4 Preisach inversion performance

Using the inverse Everett surface (see Fig.11), the hysteresis input for a demanded output can be computed. The uncompensated system response is shown in Fig.12, while the feed-forward performance is depicted in the diagram in Fig.13 for the same input signal. It can be seen that the hysteresis width is reduced, however deviations remain that can stem from

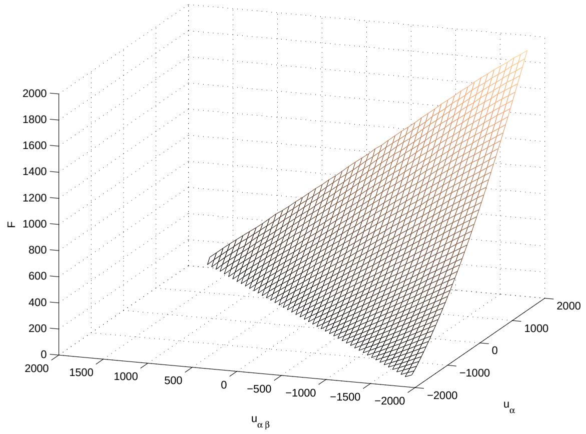

Figure 10. Averaged measured Everett-surface for the $U - F$ relation

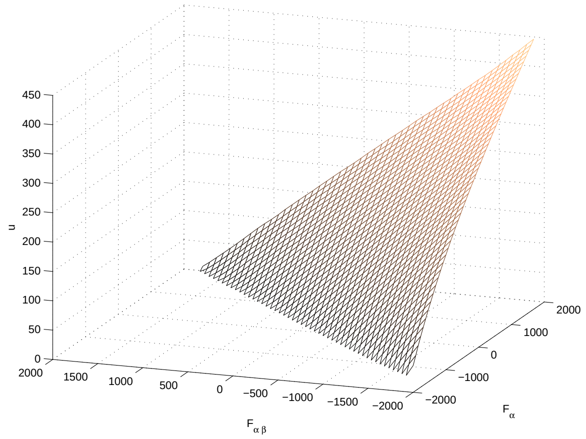

Figure 11. Inverse Everett-surface for the $U - F$ relation

system dynamics (spill-over of a higher-order structural mode), sensor dynamics, or deviating hysteresis behaviour (congruency property not exactly fulfilled). In these plots the phase lag due to the mechanical structure transfer function of $-9.6\,\mathrm{deg}$ has been subtracted, and the absolute gain has been corrected by fitting it to the reference force amplitude. Preliminary studies show that the inversion lookup computation time is small enough for real-time operation.

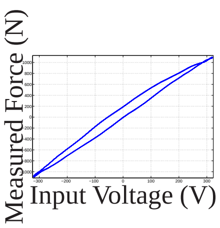

Figure 12. Raw actuator response to 10 Hz sine, phase corr.

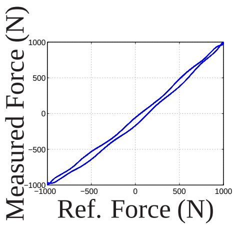

Figure 13. Actuator response to inverse signal (10 Hz sine, phase corr.)

5 Conclusion

This work showed possibilities to identify a piezoelectric stack actuator's non-linearities in a structure-mounted configuration. The Preisach hysteresis model was identified from measurement data of First-Order Descent (FOD) curves, yielding Everett surfaces by interpolation. By shaping the FOD sequence appropriately and using frequency-averaged Everett surfaces, the structure response is masked out. Measurement and experimental results are reported to support and verify the modeling and identification methodology.

For complex vibration control systems, an important sub-system is an actuator force control loop in order to track reference control force signals. This tracking performance can be improved by the proposed approach to eliminate actuator's nonlinear hysteretic behaviour using an appropriate inverse hysteresis model.

References

Ge, P. and M. Jouaneh (1996). Tracking control of a piezoceramic actuator. *IEEE Transactions on Control Systems Technology* **4**(3), 209–216.

Hu, H. and B. Mrad (2003). On the classical preisach model for hysteresis in piezoceramic actuators. *Mechatronics* **13**, 85–94.

Hughes, D. and J. T. Wen (1997). Preisach modeling of piezoceramic and shape memory alloy hysteresis. *Smart Materials and Structures* **6**, 287–300.

Kozek, M. and B. Gross (2005). Identification and inversion of magnetic hysteresis for sinusodial magnetization. *iJOE International Journal of Online Engineering - www.i-joe.org*.

Mayergoyz, I. D. (1991). *Mathematical Models of Hysteresis*. Springer. New York.

Mrad, R. B. and H. Hu (2002). A model for voltage-to-displacement dynamics in piezoceramic actuators subject to dynamic-voltage excitations. *IEEE/ASME Transactions on Mechatronics* **7**(4), 479–489.

Song, Dongwoo and C. James Li (1999). Modeling of piezo actuator's nonlinear and frequency dependent dynamics. *Mechatronics* pp. 391–410.

Yu, Y., N. Naganathan and R. Dukkipati (2002). Preisach modeling of hysteresis for piezoceramic actuator system. *Mechanism and Machine Theory* **37**, 49–59.